Progress In Electromagnetics Research B, Vol. 4, 13–25, 2008

EVALUATION OF MIMO CHANNEL CAPACITY IN INDOOR ENVIRONMENTS USING VECTOR PARABOLIC EQUATION METHOD

N. Noori † **and H. Oraizi**

Department of Electrical Engineering
Iran University of Science and Technology
Tehran 16846, Iran

Abstract—In this paper, the vector parabolic equation method (VPEM) is used to investigate the Shannon capacity of multiple-input multiple-output (MIMO) communication systems in indoor corridors. This deterministic three-dimensional (3-D) full-wave method is capable to demonstrate the effects of antennas and propagation environment on the channel capacity. The VPEM can model any field depolarization effects which are caused by the corridor walls. This method is particularly useful for evaluation of MIMO channel capacity in corridors with local narrowing of cross section. The channel capacity is computed for both single and hybrid polarizations and simulation results are compared with those obtained by the ray tracing method.

1. INTRODUCTION

Recently, the use of multiple antennas at both transmitter and receiver sites of indoor wireless communication systems has been considered as an attractive technique to increase the channel capacity without requiring extra power and bandwidth. It has been demonstrated that multiple-input multiple-output (MIMO) systems are able to offer higher capacity than their single-input single-output (SISO) counterparts. The capacity increases linearly with the number of antennas for fixed power and bandwidth [1].

In order to evaluate the capacity of an indoor MIMO system, the channel matrix of the propagation environment is required.

† Also with Department of Communications Technology, Iran Telecommunications Research Center, North Kaargar, Tehran, Iran.

This channel matrix can be determined by statistical, measurement-based or site-specific deterministic methods. Statistical approaches do not consider the dependency of the channel capacity on the exact characteristics of the radio wave propagation environment [2–4]. The measurement-based methods provide an exact model for a specific configuration but this model is not suitable to apply to other propagation environments [5, 6]. Alternatively, the site-specific deterministic methods can include the effect of the real propagation environment on the channel matrix determination. Among these deterministic techniques, the ray tracing method as a high frequency technique is the most popular one [7–11]. This method can take the characteristics of the antennas and propagation environment into account in the channel capacity calculation, but it cannot model the depolarization effect of the propagating field correctly. This depolarization which is caused by the impedance boundary conditions on the scattering objects inside the radio environment, couples energy from one field vector component to the other one. This energy coupling cannot be modeled by the Fresnel parallel and perpendicular reflection coefficients.

In this paper, the main theme and objective is to develop a model based on an unprecedented application of the vector parabolic equation method (VPEM) to evaluate MIMO system capacity inside corridors. The VPEM is a full-wave marching technique which can treat general 3-D electromagnetic problems [10]. The scalar and vector parabolic equation methods have been used as an efficient approach to compute the radar cross section of airplanes [13] and model scattering phenomena [14] and radio wave propagation in urban environment [15], troposphere [16] and Tunnels [17, 18]; however, to the authors' best knowledge it has not been used to evaluate channel capacity of MIMO systems. Application of the VPEM yields the possibility of considering all the field depolarization effects, in the channel capacity calculation. Here we study the capacity for horizontal, vertical and hybrid polarizations. The effect of narrowing the corridor cross section on the capacity of the channel is also investigated. Comparison of the VPEM numerical results with those of ray tracing method for both horizontal and vertical polarizations validates the proposed method.

2. 3-D VPEM

The VPEM has been developed for those problems which have a preferred direction of propagation (say the x-axis). We assume $e^{-i\omega t}$ time-harmonic dependence of the fields, where ω is the angular frequency. By factoring out the fast varying phase term along the x

direction, the vector electric field can be written as $\mathbf{E} = \mathbf{u}.e^{ikx}$, where k is the wave number in free space and $\mathbf{u} = (u_x, u_y, u_z)$. The 3-D parabolic equation in terms of $u = u_x, u_y, u_z$ can be expressed as [15]

$$\frac{\partial u}{\partial x} = -ik(1 - \sqrt{1 + Y + Z})u \tag{1}$$

where $Y = \partial^2/k^2\partial y^2$ and $Z = \partial^2/k^2\partial z^2$. The formal solution of (1) is given by

$$u(x + \triangle x, y, z) = e^{ik\triangle x(\sqrt{1+Y+Z}-1)}u(x, y, z). \tag{2}$$

For numerical implementation, we need a suitable approximation of the exponential operator. The first order Taylor expansion of the square-root operator yields the following approximation for (2)

$$u(x + \triangle x, y, z) = e^{\frac{ik\triangle x}{2}Y}e^{\frac{ik\triangle x}{2}Z}u(x, y, z). \tag{3}$$

This equation corresponds to the well-known standard parabolic equation (SPE)

$$\frac{\partial u}{\partial x} = \frac{i}{2k}\left(\frac{\partial^2 u}{\partial y^2} + \frac{\partial^2 u}{\partial z^2}\right). \tag{4}$$

The SPE is known to be valid at angles within 15° of the horizontal axis (the positive direction of the x-axis). For better stability properties, we can apply the Padé (1,0) approximations of the exponential operators in (3) which result in the following equation

$$\left(1 - \delta\frac{Y}{2}\right)\left(1 - \delta\frac{Z}{2}\right)u(x + \triangle x, y, z) = u(x, y, z) \tag{5}$$

where $\delta = ik\Delta x$. This finite-difference equation must be written for each field component, resulting in three scalar parabolic equations. These scalar equations are coupled through the impedance boundary conditions on the corridor walls [20, ,21]

$$\mathbf{n} \times \mathbf{E} = \frac{1}{ik\sqrt{\epsilon_r}}\mathbf{n} \times (\mathbf{n} \times \nabla \times \mathbf{E}) \tag{6}$$

where ϵ_r is the wall relative permittivity and $\mathbf{n}$ is the outward unit vector onto the surface of the scattering objects located in the propagation environment. It can be seen that these impedance boundary conditions couple energy from one field vector component to the other one. This depolarization effect cannot be considered even by

advanced ray tracing methods. Equation (6) contains two independent scalar equations; therefore, we need the divergence-free condition of Maxwell's equations to obtain a system of rank 3

$$\nabla \cdot \mathbf{E} = \nabla \cdot (\mathbf{u}e^{ikx}) = 0. \tag{7}$$

In (6) and (7) the first order derivative with respect to x is replaced by its equivalent form Equation (4). The resulting general marching algorithm is devised for the three dimensional VPEM, whereby the field at step $x_0 + \triangle x$ is computed by that at x_0. This technique can be used to simulate radio wave propagation inside the environment and correctly models the field polarization effects.

3. CAPACITY CALCULATION

The VPEM is used to compute the received field at all receiver locations in the whole propagation domain in the case of one transmitting antenna. In a MIMO system with N_T transmitting and N_R receiving antennas, this process is repeated for each transmitting antenna to obtain the channel matrix $\mathbf{G}$. The matrix $\mathbf{G}$ is a $N_R \times N_T$ matrix and the element G_{nm} is the received field at antenna n while only antenna m is transmitting. It is assumed that the channel is narrow-band with no frequency dependence and the noise is additive white Gaussian. The channel capacity of this MIMO system with an average received SNR (ρ) at each receiving antenna has been obtained in b/s/Hz as [1]

$$C = \log_2 \left[\det \left(\mathbf{I}_{N_R} + \frac{\rho}{N_T} \mathbf{H}\mathbf{H}^* \right) \right] \tag{8}$$

where $\mathbf{I}$ is the identity matrix, $\mathbf{H}$ is the $N_R \times N_T$ normalized channel matrix and $\mathbf{H}^*$ is the Hermitian (complex conjugate transpose) of $\mathbf{H}$. The normalized channel matrix is obtained by performing the Frobenius norm on $\mathbf{G}$

$$\mathbf{H} = \frac{\mathbf{G}}{\sqrt{\frac{\sum_{n=1}^{N_R} \sum_{m=1}^{N_T} |G_{n,m}|^2}{N_T N_R}}}. \tag{9}$$

Singular value decomposition can be used to resolve the channel into a set of independent sub-channels and applying the channel capacity theorem to each one of them [9, 22, 23]. In this case the capacity can be calculated by

$$C = \sum_{i=1}^{K} \log_2 \left(1 + \lambda_i \frac{\rho}{N_T} \right) \tag{10}$$

where λ_i's are the eigenvalues [24, 25] of $\mathbf{HH}^*$ and K is the rank of $\mathbf{H}$ and is equal to $\min(N_R, N_T)$. It should be noted that the matrix $\mathbf{H}$ is normalized to remove the path loss component so it only shows the relative variation of the path response from each transmitting to each receiving antenna [1]. Therefore, there is no correlation between the channel capacity and received power. The channel capacity is determined by the correlation among sub-channels. The lower correlation causes the higher capacity.

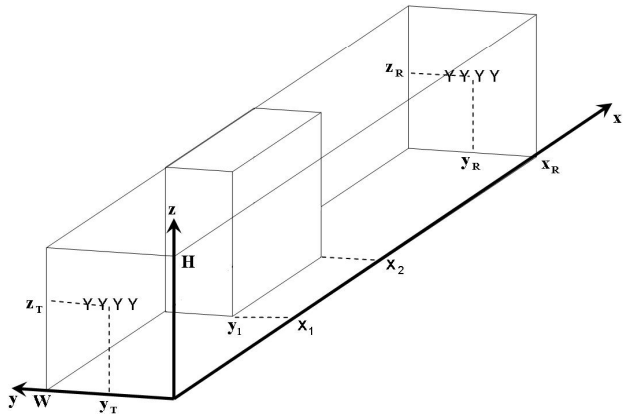

Figure 1. Geometrical configuration of the corridor.

4. SIMULATION RESULTS

For numerical simulation, we consider a corridor with 15λ width, 18λ height and 600λ length which would correspond to a $2.5\,\mathrm{m} \times 3\,\mathrm{m} \times 100\,\mathrm{m}$ corridor at the operating frequency of 1.8 GHz as shown in Fig. 1. The corridor walls have a complex dielectric constant of $\epsilon_{cr} = \epsilon_r - i60\sigma\lambda$ with $\epsilon_r = 4$ and $\sigma = 0.02\,\mathrm{S/m}$, while the ceiling and floor are modeled by $\epsilon_r = 6$ and $\sigma = 0.05\,\mathrm{S/m}$. Assume a 4×4 MIMO system where the transmitting and receiving linear arrays are arranged horizontally in the y direction. The center of the transmitting array is fixed at $(x_t, y_t, z_t) = (0, 1.25\,\mathrm{m}, 2.25\,\mathrm{m})$ and it consists of $\lambda/2$ separated Gaussian pencil beam source antennas where each antenna element has a beam width of 10°. The pencil beam is directed towards the preferred direction of propagation (for example along the corridor axis as the paraxial direction). It should also be noted that the pencil beam does not have appreciable side lobes. This is appropriate for modeling wave propagation in the corridor medium by the parabolic equation

method. The mutual coupling among [26] the narrow beam Gaussian antennas is negligible and can be neglected. The antenna element spacing of the receiving array is $\lambda/2$ and the required average SNR at each receiver antenna element is taken to be constant and equal to 20 dB which is a reasonable value for a wireless system.

We start the field computation just after the transmitter along the x direction. The propagating field is computed on a sequence of cross-sectional parallel planes by marching algorithm, applying the impedance boundary conditions on the walls, ceiling and floor. Since it is assumed that the radiation pattern of the antenna has a pencil beam, the electromagnetic field amplitudes and power levels are quite low outside the paraxial direction, therefore, the impedance boundary condition can be used [12]. We continue these computations until the wave reaches the front wall of the corridor. By applying the impedance boundary condition on the corridor cross-sectional front wall, the reflected field is obtained. Then the initial field is set equal to this reflected field and the marching algorithm is started in the reverse direction ($-x$). The algorithm is continued upto the back wall of the corridor. The total field is the summation of calculated fields in the two directions. By applying the impedance boundary conditions, on the back wall, the reflected field is obtained. This process is continued until the computed field in one marching direction falls below a threshold level.

4.1. A Corridor with Constant Cross Section

The receiving array moves horizontally along the $(x_r, y_r, z_r) = (x_r, 1.25\,\text{m}, 1.75\,\text{m})$. To validate the method, the average received power is calculated by VPEM and compared with the ray tracing method in Figs. 2 and 3, where the transmitting and receiving antennas are both vertically (VV) or horizontally (HH) polarized. To obtain these results the reflected waves from the front and back walls of the corridor are neglected. As can be seen, the results of the VPEM are very close to those obtained by the ray tracing method. The differences originate from different features of these methods in employing the boundary conditions. The multipath effect of the wave propagation causes fading and variation of the received signal along the length of the corridor.

In Figs. 4 and 5, the received power is obtained by taking into account the reflected waves from both the front and back walls for VV and HH polarizations, respectively and are compared with the case where the back wall reflections are neglected. It can be seen that the two power curves coincide with each other and the reflected wave from the back wall does not have any significant effect on the received

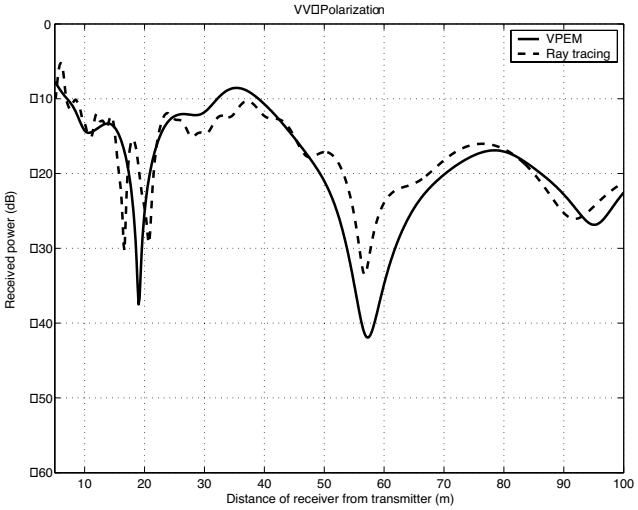

Figure 2. Received power for VV polarization versus receiver location neglecting front and back walls reflections.

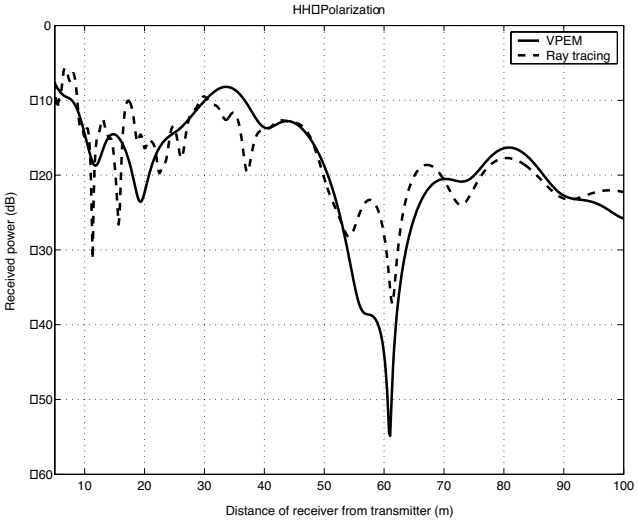

Figure 3. Received power for HH polarization versus receiver location neglecting front and back walls reflections.

power. For convenience, we obtain the next results by considering only reflection from the front wall.

Figure 6 shows the average received power for cross-polarized

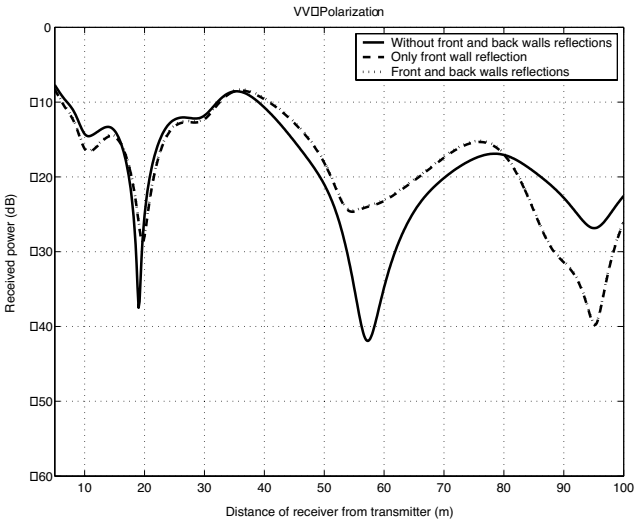

Figure 4. Received power for VV polarization versus receiver location.

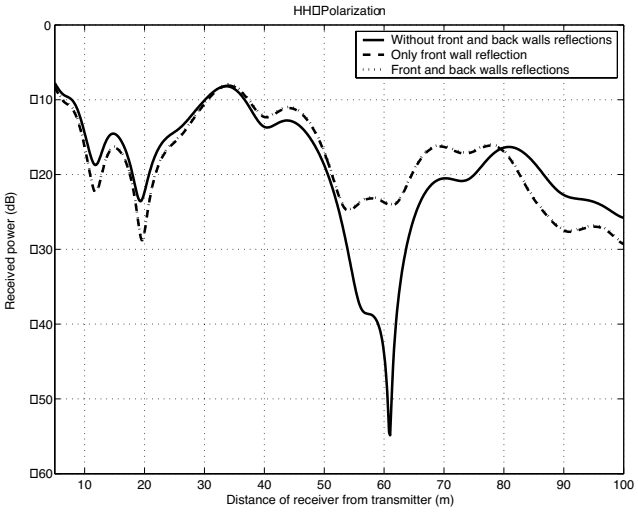

Figure 5. Received power for HH polarization versus receiver location.

transmitter-receiver antennas (VH and HV cases) and compare the results with VV and HH cases. It can be seen that the cross-polarization coupling is at the level of $-20\,\mathrm{dB}$. This coupling is due to the reflections from walls, ceiling and floor. As it is mentioned, this

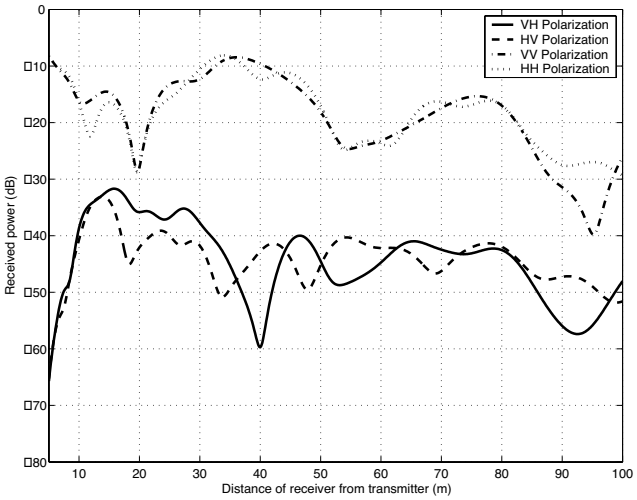

Figure 6. Received power for VH and HV polarizations versus receiver location by considering only front wall reection.

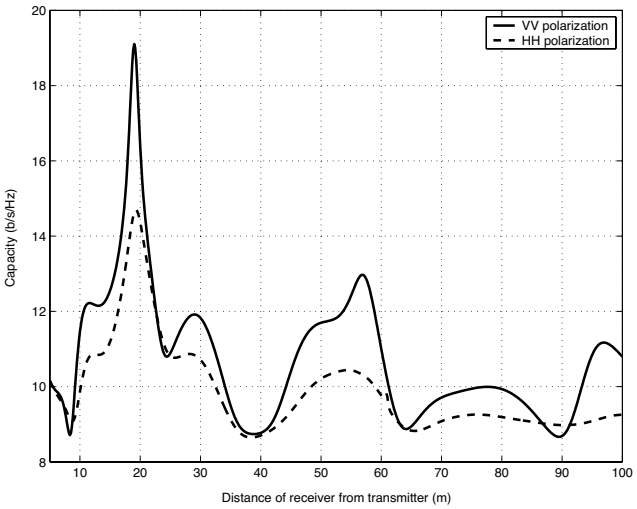

Figure 7. MIMO channel capacity for VV and HH polarizations versus receiver location by considering only front wall reflection.

depolarization is caused by the impedance boundary conditions and cannot be modeled by the ray tracing method.

Figure 7 shows the channel capacity of the above mentioned

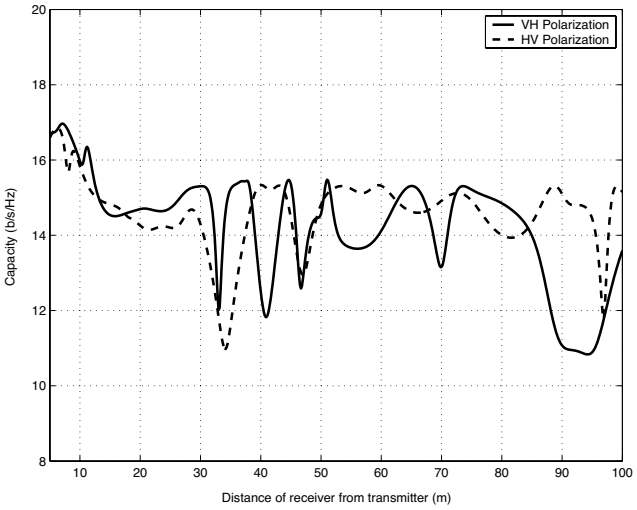

Figure 8. Comparison of the MIMO channel capacity for VH and HV polarizations by considering only front wall reflection.

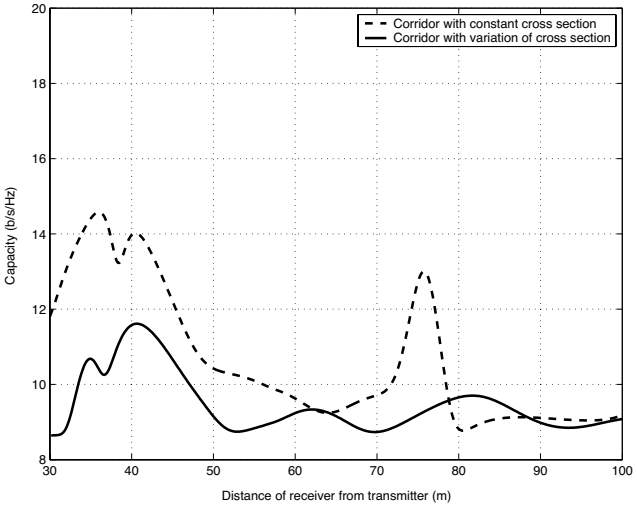

Figure 9. MIMO channel capacity of a corridor with local narrowing of cross section in comparison with the capacity of a constant cross section corridor.

MIMO system for VV and HH cases. It can be observed that, in this corridor, the vertically polarized system achieves higher capacity than its horizontally polarized counterpart. Fig. 8 shows the channel

capacity variation along the corridor for VH and HV configurations. By comparison between Figs. 7 and 8, it can be observed that for most of the receiver array locations, HV and VH (hybrid polarizations) systems show higher channel capacity than VV and HH systems. In practice, in these cases, 20 dB more power is required to reach the same SNR. It should be noted that in hybrid polarization cases, the channel capacity increases due to the reduction of the sub-channel correlations..

4.2. A Corridor with Variation of Cross Section

Assume that the corridor in Fig. 1 has a width reduction at a distance of 20 m from the transmitter where the corridor width reduces to 1.5 m. Then the corridor width increases to its initial value of 2.5 m at 30 m from the transmitter. The receiver moves in the corridor along the $(x_r, y_r, z_r) = (x_r, 2\,\mathrm{m}, 1.75\,\mathrm{m})$, therefore this width reduction obstructs the line of sight (LOS) path for many receiving locations. Fig. 9 shows the channel capacity for a VV system. It can be seen that, the channel capacity decreases significantly for those receiving locations where the LOS path is obstructed.

5. CONCLUSIONS

In this paper, a new full-wave analytical approach based on the vector parabolic equation method has been proposed for estimating the channel capacity of MIMO systems in a corridor environment. This full-wave VPEM method is capable of considering the effect of actual propagation environment for channel capacity calculation. The proposed method is able to model the antenna polarization correctly and can be applied to any furnished corridor with variation of cross section.

REFERENCES

1. Foschini, G. J. and M. J. Gans, "On limits of wireless communications in a fading environment when using multiple antennas," *Wireless Personal Communications*, Vol. 6, 311–335, 1998.
2. Chunyan, G., Z. Ming, Z. Shidong, and Y. Yan, "A new calculation on the mean capacity of MIMO systems over Rayleigh fading channels," *Proc. IEEE 14th Int. Symp. Personal, Indoor, and Mobile Radio Communications*, Vol. 3, 2267–2270, 2003.
3. Khalighi, M. A., J. M. Brossier, G. Jourdain, and K. Raoof, "On capacity of Rician MIMO channels," *Proc. IEEE 12th Int. Symp.*

Personal, Indoor, and Mobile Radio Communications, Vol. 1, 150–154, 2001.

4. Yarkoni, N. and N. Blaunstein, "Prediction of propagation characteristics in indoor radio communication environments," *Progress In Electromagnetics Research*, PIER 59, 151–174, 2006.
5. Kyritsi, P., D. C. Cox, R. A. Valenzuela, and P. W. Wolniansky, "Effect of antenna polarization on the capacity of a multiple element system in an indoor environment," *IEEE J. Select. Areas Commun.*, Vol. 20, No. 6, 1227–1239, 2002.
6. Eugene, C. H. Y., K. Sakaguchi, and K. Araki, "Experimental and analytical investigation of MIMO channel capacity in an indoor line-of-sight (LOS) environment," *Proc. IEEE 15th Int. Symp. Personal, Indoor, and Mobile Radio Communications*, Vol. 1, 295–300, 2004.
7. Oh, S. H. and N. H. Myung, "MIMO channel estimation method using ray-tracing propagation model," *Electron. Lett.*, Vol. 40, No. 21, 311–335, 2004.
8. Elnaggar, M., S. Safavi-Naeini, and S. K. Chaudhuri, "Effect of oversimplifying the simulated indoor propagation on the deterministic MIMO capacity," *Proc. Canadian Conference on Electrical and Computer Engineering*, Vol. 1, 219–222, 2004.
9. Burr, A., "Evaluation of capacity of indoor wireless MIMO channel using ray tracing," *Proc. International Zurich Seminar on Communications*, 28-1–28-6, 2002.
10. Chen, C. H., C. L. Liu, C. C. Chiu, and T. M. Hu, "Ultra-wide band channel calculation by SBR/image techniques for indoor communication," *Journal of Electromagnetic Waves and Applications*, Vol. 20, No. 1, 41–51, 2006.
11. Teh, C. H., F. Kung, and H. T. Chuah, "A path-corrected wall model for ray-tracing propagation modeling," *Journal of Electromagnetic Waves and Applications*, Vol. 20, No. 2, 207–214, 2006.
12. Zaporozhets, A. A. and M. F. Levy, "Bistatic RCS calculations with the vector parabolic equation method," *IEEE Trans. Antennas Propagt.*, Vol. 47, No. 11, 1688–1696, 1999.
13. Mallahzadeh, A. R., M. Soleimani, and J. Rashed-Mohassel, "RCS computation of airplane using parabolic equation," *Progress In Electromagnetics Research*, PIER 57, 265–276, 2006.
14. Graglia, R. D., G. Guarnieri, G. Pelosi, and S. Selleri, "The parabolic equation method for the high-frequency scattering from a convex perfectly conducting wedge with curved faces," *J. of Electromagnetic Waves and Appl.*, Vol. 21, No. 5, 585–598, 2007.

15. Zaporozhets, A. A., "Application of vector parabolic equation method to urban radiowave propagation problems," *Proc. Inst. Elect. Eng. Microwaves, Antennas Propagat.*, Vol. 146, No. 4, 253–256, 1999.
16. Awadallah, R. S., J. Z. Gehman, J. R. Kuttler, and M. H. Newkirk, "Effects of lateral terrain variations on tropospheric radar propagation," *IEEE Trans. Antennas Propagt.*, Vol. 53, No. 1, 420–434, 2005.
17. Noori, N., S. Safavi-Naeini, and H. Oraizi, "A new three-dimensional vector parabolic equation approach for modeling radio wave propagation in tunnels," *Proc. International Symposium on Antennas and Propagat.*, Vol. 4B, 314–317, 2005.
18. Oraizi, H. and N. Noori, "Least square solution of the 3-D vector parabolic equation," *Journal of Electromagnetic Waves and Applications*, Vol. 20, No. 9, 1175–1178, 2006.
19. Levy, M. F., *Parabolic Equation Methods for Electromagnetic Wave Propagation*, IEE, U.K., 2000.
20. Senior, T. B. A. and J. L. Volakis, *Approximate Boundary Conditions in Electromagnetics*, IEE, U.K., 1995.
21. Zhang, P. F. and S. X. Gong, "Improvement on the forward-backward iterative physical optics algorithm applied to computing the RCS of large open-ended cavities," *Journal of Electromagnetic Waves and Applications*, Vol. 21, No. 4, 457–469, 2007.
22. Abouda, A. A., H. M. El-Sallabi, and L. Vuokko, "Spatial smoothing effects on Kroneker MIMO channel model in urban microcells," *Journal of Electromagnetic Waves and Applications*, Vol. 21, No. 5, 681–696, 2007.
23. Abouda, A. A., H. M. El-Sallabi, and S. G. Hägman, "Effect of antenna array geometry and ula azimuthal orientation on MIMO channel properties in urban city street grid," *Progress In Electromagnetics Research*, PIER 64, 257–278, 2006.
24. Chen, X., "Time-reversal operator for a small sphere in electromagnetic fields," *Journal of Electromagnetic Waves and Applications*, Vol. 21, No. 9, 1219–1230, 2007.
25. Angiulli, G., "On the computation of nonlinear eigenvalues in electromagnetic problems," *Journal of Electromagnetic Waves and Applications*, Vol. 21, No. 4, 527–532, 2007.
26. Abouda, A. A., and S. G. Hägman, "Effect of mutual coupling on capacity of mimo wireless channels in high SNR scenario," *Progress In Electromagnetics Research*, PIER 65, 27–40, 2006.